HIGH-RESOLUTION LIQUID-FILLED MULTI-WIRE CHAMBERS FOR USE IN HIGH-ENERGY BEAMS

S. E. Derenzo, A. Schwemin, R. G. Smits,
H. Zaklad, and L. W. Alvarez

Lawrence Berkeley Laboratory
University of California
Berkeley, California 94720

ABSTRACT

We describe experiments with liquid-xenon-filled wire chambers operating in the proportional mode and the difficulty of achieving useful gain when the anode wires have a spacing < 1 mm. As a result, we have largely turned our attention to chambers with closely spaced wires operated in the ionization mode. We have previously demonstrated a spatial resolution of 15 μ rms in this mode, using a 5-wire chamber and a collimated alpha source.

We describe the construction of two small high-resolution test chambers to be filled with liquid argon, krypton, or xenon. The chambers consist of two flat cathodes 1 to 2.5 mm apart with a wire plane between them. The wire plane is an array of 24 wires, 5 μ in diameter, spaced on 20-μ centers, and a charge amplifier is attached to each wire. The space resolution (expected rms < 20 μ), time resolution (expected rms < 50 ns), and efficiency will be measured in an accelerator beam. Chambers of this type with only a few hundred wires have sufficient area to cover nearly every beam at NAL.

1.-INTRODUCTION

For several years, following a suggestion by Luis Alvarez[1], we have been studying the use of liquified noble gases for particle detection. Two types of wire chambers are emerging: one type having high spatial resolution for high-energy physics[2-3] and the other type having a unique combination of size, spatial resolution, energy resolution, and gamma-ray detection efficiency for nuclear medicine[4-5].

In Section 2 we discuss what we have learned about the avalanche of electrons in liquid xenon, both in single-wire and multi-wire proportional chambers. In Section 3 we discuss the construction of high-resolution liquid-filled multi-wire ionization chambers for use in high-energy beams.

2.-ELECTRON AVALANCHE IN LIQUID XENON

2.1.-Single-Wire Proportional Chambers

We have learned much from these simple chambers (see Fig. 1, Ref. 3): (i) the electron avalanche in liquid argon has low reliability, low detection efficiency, and the pulses are in general not proportional to the initial ionization[6], (ii) the electron avalanche in liquid xenon is highly reliable, has ~100% detection efficiency, and the pulses are proportional to the initial ionization, (iii) liquid xenon can be prepared free from nearly all electronegative contaminants by use of a specially designed noble gas purifier[7] and by the use of field emission electrons from the fine central electrode to ionize impurities and sweep them to the outer electrode[4].

In addition, we have taken data of pulse height vs applied voltage for 2.9-, 3.5-, and 5.0-μ diameter anode wires (see Fig. 2, Ref. 3) and these data vary by < 10% from one chamber filling to another. The electron avalanche has an exponential growth and the characteristic distance for that growth is $1/\alpha$, where α is the first Townsend coefficient. By comparing pulse heights between chambers having somewhat different anode diameters, it is possible to derive α as a function of electric field E. In fact, we performed a χ^2 fitting of a single function $\alpha(E)$ to the data for all three wires[8]. The result is plotted in Fig. 1 as $\eta = \alpha/E$ vs E/ρ (ρ = density) and compared with corresponding values measured in xenon gas[9-10]. We conclude that electrons avalanche in liquid xenon as they would in xenon gas at a density of 120 g/liter rather than the liquid density of 3057 g/liter.

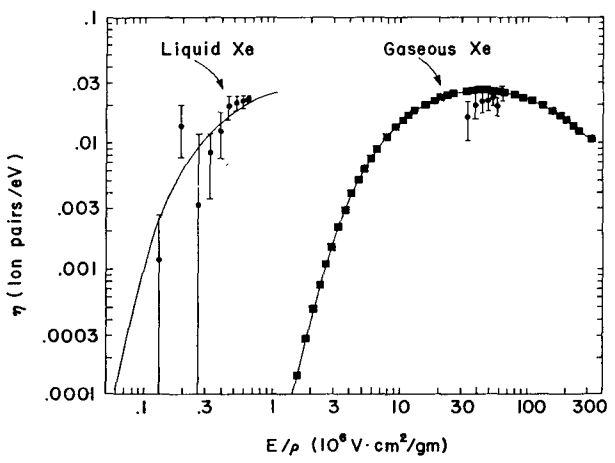

Fig. 1. Avalanche ionization coefficient $\eta = \alpha/E$ vs E/ρ for gaseous and liquid xenon, where α is the first Townsend coefficient (the inverse of the ionization mean free path), E is the electric field, and ρ is the density. (See Ref. 8 for details)

We have used the function $\alpha(E)$ measured in liquid xenon to predict the pulse-height-vs-voltage curve measured in solid xenon by Pisarev et al.[11]. The agreement is very good, indicating that $\alpha(E)$ is nearly identical in both liquid and solid xenon.

These same authors also measured pulse height vs voltage in the same chamber, using a gaseous xenon filling at pressures ranging from 1 to 50 atm[12]. Their solid-xenon curve agrees best with

their gaseous-xenon curve for 30 atm, showing the remarkable fact that a single-wire proportional chamber filled with 30 atm xenon ($\rho \approx 240$ g/liter) requires approximately the same operating potential (2 to 4 kV) as the same chamber filled with solid xenon ($\rho = 3540$ g/liter).

2.2. -Multi-wire Proportional Chambers

2.2.1. -Gamma-Ray Chambers. We have achieved proportional gains up to 50 in a 24-wire chamber 2 cm thick to be used for the imaging of distributions of gamma-ray emitters[5]. The wires are 5 μ in diameter and spaced 2.8 mm apart (see Fig. 6 of Ref. 3). In Fig. 2 we compare pulse height vs voltage for the single-wire proportional chamber and the 24-wire proportional chamber. Allowing for the different geometries (i.e., different voltage scale factors), the agreement is excellent.

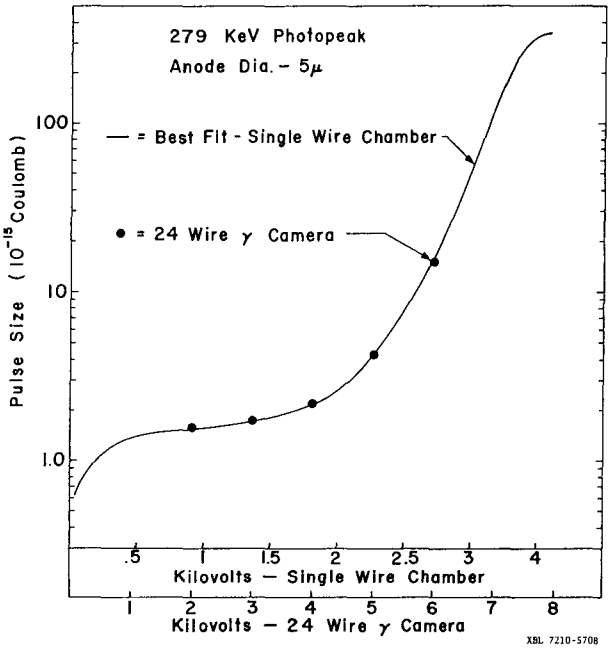

Fig. 2. Pulse height vs voltage for 5-μ wire. Solid curve: data from single-wire chamber; dots: data from 24-wire proportional chamber. Due to differences in geometry, the voltage scales differ by a factor of 2.2.

Due to the low wire tensions (1.6 g) and large potentials applied to this chamber (~ 5000 V), we found it necessary to support the wires with pairs of quartz fibers. Initially, we used 1, 2, and even 3 pairs of 400-μ-diameter fibers and in every case found 1- to 2-cm-wide regions of greatly reduced gain at each pair of fibers. When the fiber diameter was reduced to 50 μ these dead regions were no longer noticeable.

This is a striking demonstration, showing that any insulator near a region of electron avalanche charges up (presumably with diffusing Xe^+ ions) and reduces the electric field on nearby wires.

This chamber has been used with a charge-division readout circuit on both the anode wires and cathode strips to record distributions of gamma rays[5]. In Fig. 3 we show the image of the letters "XE" formed by 279-keV gamma rays passing through slots in a lead block and interacting in the chamber.

Fig. 3. Image of the letters "XE" cut into a lead collimator as recorded in the 24-wire liquid xenon multi-wire proportional chamber, using 279-keV gamma rays.

2.2.2. Amplification on Closely Spaced Wires. We hoped that the amplification factors achieved in the single-wire chambers (up to 1500 when using 0.1% ethylene in liquid xenon—see Fig. 5 of Ref. 3) could be realized for arrays of fine, closely spaced wires. The chamber shown in Fig. 4 was constructed to measure amplification as a function of voltage and spacing. We used well-polished stainless steel cathodes oxidized in room air. Swan and Lewis showed that such cathodes provided an electric strength in excess of 1.6×10^6 V/cm in liquid argon—higher than any other material they tested[13]. The 3.5-μ-diameter tungsten anode wires were stretched across a hole in the stainless steel anode plate and spot-welded to it. To avoid excessive fields at the edge wires, the fine anode wires were placed between two larger 20-μ-diameter stainless steel wires. The anode plate was secured with a spring clip to allow for a convenient exchange with anodes of different wire spacings. The cathode plates were 4.4 mm apart, and the anode plate was centered between them. An ^{241}Am source was rubbed against one cathode to provide a source of alpha particles without significantly affecting the polished condition of the cathode.

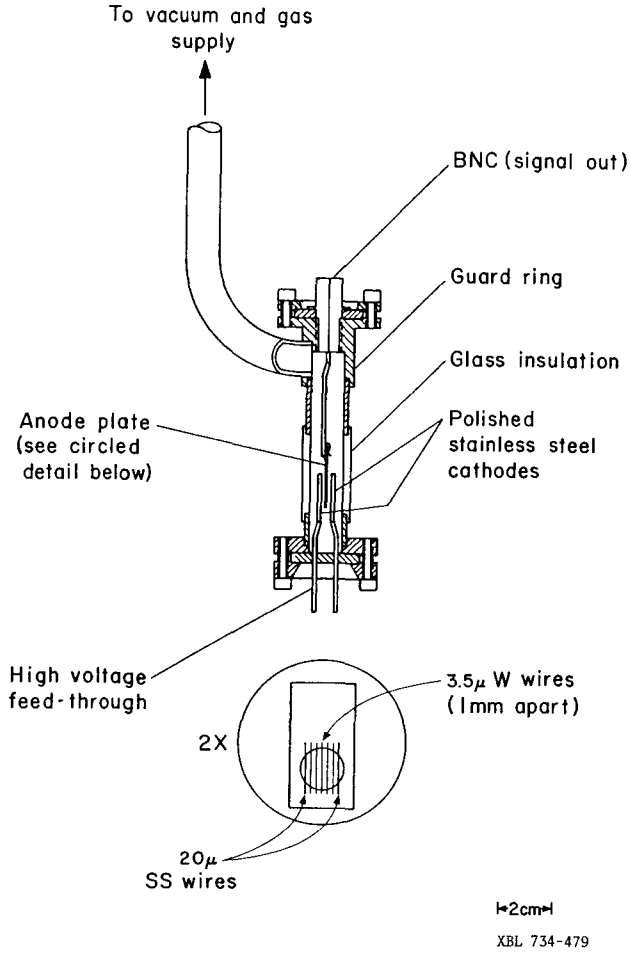

Fig. 4. Multi-wire test chamber. Cathodes are polished stainless steel plates, one containing an ^{241}Am source. Anode is a stainless steel plate with 3.5-μ-diameter wires stretched across a hole.

When using wire spacings of 150 and 300 μ, amplification was not observed. The operating voltage was limited to 9 kV by sparking between the cathode and one of the 3.5-μ-diameter anode wires, frequently resulting in its breakage. At 9 kV and 150-μ spacing, the anode field was 1.06×10^6 V/cm and the cathode field was 39 kV/cm[14]. At 9 kV and 300-μ spacing, the anode field was 2.0×10^6 and the cathode field was 36 kV/cm. Below the sparking potential a large number of pulses of irregular shape and size were seen. For the 1-mm wire spacing (shown in Fig. 4) a gain of 10 was observed at 5000 V. Above this voltage, sparking again occurred between cathode and anode. The sparks were surprising, because the cathode field was a mere 13.8 kV/cm. The anode field, however, was 2.5×10^6 V/cm.

2.2.3. Possibilities for High Spatial Resolution over Large Areas. Useful gain (> 100) on closely spaced wires in liquid xenon would make large area chambers quite practical. We are considering the following possibilities:

(1) well oxidized cathodes and carefully de-oxidized anodes to reduce spark breakdown (see Ref. 13),

(2) dissolved ethylene or carbon dioxide to absorb the uv emitted by excited Xe atoms and prevent regenerative breakdown leading to sparks, and

(3) wire significantly finer than 3.5 μ to increase the ratio between anode and cathode fields.

(4) The use of solidified argon or xenon, which appear attractive in that:

(a) the wires are frozen in place, eliminating electromechanical instabilities and

(b) these solids are reported to have hole conduction, resulting in larger positive ion mobilities and less space charge. However, it appears unlikely that the multi-wire spark breakdown will occur in pure solid xenon at significantly different fields than in pure liquid xenon. Moreover, the preparation of large crystals (> 5 cm) pure enough and sufficiently free from defects for useful electron and hole transport is difficult even for such well-researched materials as germanium.

If gains in excess of 100 are possible only on wires spaced ≥ 500 μ apart, then high spatial resolution might still be achieved by accurately finding the center of the charge induced at the cathode. An analog shift register might be used to periodically transfer the charge from each cathode strip to an analog-to-digital converter. The center of charge might subsequently be calculated in a digital computer with considerable precision.

3. -HIGH-PRECISION MULTI-WIRE LIQUID-FILLED IONIZATION CHAMBERS

3.1. -Motivation

Realizing that amplification on closely spaced wires is not at hand, we are building and testing small chambers having very closely spaced wires (20 μ apart) and a charge amplifier on each wire to compensate for the lack of amplification in the liquid. Two chambers will be placed as close as possible (anode planes 2 to 4 mm apart) in a Bevatron beam with the wires in one chamber parallel to those in the other. The objectives of this test are a measurement of space resolution (using one chamber to check the other), time resolution, and efficiency. Such chambers are well-suited for use in the small-diameter high-energy charged beams at NAL. In this application an amplifier on each wire would be desired in any case for maximum rate: the lack of amplification in the liquid increases the amplifier cost but does not limit any characteristic of the chamber (except, perhaps, size).

Such chambers could be used in conjunction with a 15-kG meter magnetic dipole to form a spectrometer 2 meters long yet capable of measuring the momentum of 150-GeV/c hyperons, for example, to an accuracy of ± 2%.

3.2. - Expected Characteristics

In Table I we list selected properties of liquid Ar, Kr, and Xe, and in Table II we list the characteristics expected for multi-wire ionization chambers filled with these liquids.

The pulse size amounts to one-half of the free electrons produced in the chamber because, on the average, the electrons drift through only half the available potential[15]. The Xe^+ ions drift too slowly to contribute to the pulse.

We have defined the pulse rise time to be the electron drift time from the cathode to the anode plane. A graph showing electron drift velocities vs electric field for all liquified noble gases and many room temperature hydrocarbons may be seen in Fig. 9 of Ref. 8. The electron drift velocities in solid Xe, Kr, and Ar are 2 to 3 times higher than in the liquids[16].

The time resolution σ_t (limited primarily by amplifier noise) is given approximately by

$$\sigma_t = \left(\frac{2N}{S}\right) \tau,$$

where S/N is the signal-to-noise ratio and τ is the rise time of the filtered pulse. Since N increases slowly with increased bandwidth B but $\tau \propto 1/B$, the time resolution is optimized when the amplifier pulse-shaping rise time is equal to the pulse rise time. Increasing the chamber thickness increases the signal S and pulse rise time τ by equal amounts so that σ_τ is not a strong function of chamber thickness. Note that τ/S is smaller for liquid xenon than for liquid argon or krypton.

The spatial resolution is limited by the production of delta rays and the diffusion of electrons, described below.

The cross section σ for producing a delta ray of kinetic energy $T > T_{min}$ by a fast track is given by[19]

$$\sigma = \frac{250 \text{ keV barn}}{T_{min}}.$$

Therefore, the probability P that a fast track—while traversing a layer of thickness d—will produce a delta ray having kinetic energy $T > T_{min}$ is given by

$$P = 1 - e^{-Kd/T_{min}},$$

TABLE I. Selected properties of liquid Ar, Kr, and Xe.[a]

Property	Ar	Kr	Xe
Boiling point at 1 atm (°C)	-185.9	-153.4	-108.1
Melting point[b] (°C)	-189.4	-157.2	-111.8
Liquid density (boiling at 1 atm) (g/cm^3)[c]	1.400	2.413	3.057
STP gas/boiling liquid (1 atm) volume ratio	784.0	643.6	518.9
^{85}Kr decays/s/cm^3[d]	0	400	8×10^{-3}
Electron drift velocity at 1 kV/cm(10^5cm/s)	2.4	2.4	2.4
Electron drift velocity at 10 kV/cm(10^5cm/s)	5.0	4.0	2.8
Radiation length (cm)	13.5	4.6	2.6
Collision length (cm)	65	48	44
dE/dX (minimum) (MeV/cm)	2.25	3.4	3.9
Av ionization potential (eV/pair)	26.4	24.3	21.9
Cost per liquid liter (U. S. A.$)	0.25	700	2000

[a] Thermodynamic properties from Ref. 17. Electron drift velocities from Ref. 16.

[b] Changes very slowly with pressure.

[c] The densities of melting Ar, Kr, and Xe are 1.623, 2.826, and 3.540 g/cm^3, respectively.

[d] Atmospheric "pollution" due to nuclear reactors (see Ref. 18). Typical Kr concentration in commercial Xe is 20 ppm.

TABLE II. Liquid-filled multi-wire ionization chambers.[a]

Characteristic	Ar	Kr	Xe
Chamber thickness for 10 000 e^- pulses (mm)	2.4	1.4	1.1
Energy loss (keV)	528	486	438
Pulse rise time[b] (ns)	250	175	165
Time Resolution[c] (ns)	±60	±45	±40
Radiation length[d] (fraction)	0.019	0.031	0.043

[a]Anticipated characteristics for chambers having a thickness such that minimum ionization tracks produce an average of 20 000 ion pairs. The charge pulse received is 10 000 e^-.

[b]Electron drift time for 1/2 chamber thickness, assuming $E = 10^4$ V/cm. For solid Ar, Kr, Xe these numbers are 85, 70, and 95 ns, respectively.

[c]Taking under consideration the rise time and the corresponding amplifier signal-to-noise ratio. See text, Sections 3.2 and 3.4 for details.

[d]Note that 250 μ stainless steel is 0.014 radiation lengths and 500 μ Mylar is 0.001 radiation lengths. The transverse momentum uncertainty (rms) due to multiple scattering for 250 μ stainless steel plus 500 μ Mylar plus the thickness of liquid Ar, Kr, or Xe shown above is 2.8, 3.2, and 3.6 MeV/c, respectively.

where K = 9.5 keV/mm in liquid argon,
K = 15.5 keV/mm in liquid krypton,
and K = 19 keV/mm in liquid xenon.

Assuming a value P = 0.2 and the values of d given in Table II,

T_{min} = 102 keV for liquid argon,
T_{min} = 97 keV for liquid krypton,
and T_{min} = 94 keV for liquid xenon.

Thus, in all three of the chambers shown in Table II, a fast particle will produce a delta ray of kinetic energy T > 100 keV with a probability of 20%.

In liquid xenon, a 100-keV electron suffers severe multiple scattering and although it travels 90 μ, its end point is (on the average) 12 ±5 μ from its point of origin[20]. A one-dimentional projection of origin-to-end-point vectors has an rms of 7.5 μ. Thus, the delta-ray ionization resembles a diffuse cloud rather than a track. In liquid argon we expect these lengths to increase threefold. Liquid krypton should be an intermediate case.

Tracks with delta rays having kinetic energy >100 keV can be identified (and even rejected) by the number of wires receiving a significant pulse.

The diffusion of electrons in liquids cannot be calculated precisely, because neither the diffusion constant nor the agitation energy have ever been measured for any liquid. However, the ratio of the diffusion coefficient D to the mobility coefficient μ has been measured for electrons in gaseous argon by Warren and Parker[21]. They found $D/\mu = 1$ V at $E/P = 1.68 \times 10^{-2}$ V/cm/Torr (E/P = the ratio of the electric field to gas pressure).

In the 2.4-mm liquid argon chamber of Table II, the electrons travel in a field $E = 10^4$ V/cm ($E/P = 1.68 \times 10^{-2}$ V/cm/Torr) an average distance 0.6 mm at a drift velocity $v_d = 5 \times 10^5$ V/cm (mobility $\mu = v_d/E = 50$) for a time t = 125 ns. We may tentatively estimate the rms lateral electron diffusion:

$$\sigma_x = \sqrt{2Dt} \approx 35\ \mu.$$

A measurement (or upper limit) of σ_x vs E is one of the objectives of the Bevatron test.

We have previously measured the spatial resolution for a 700-μ-thick liquid xenon chamber having 5-μ wires on 50-μ centers, using a collimated alpha source[22] and found it to be < 15 μ rms[2]. This test indicates that electron diffusion in liquid xenon is less than that predicted by the above estimate for liquid argon, based on diffusion measurements in the gas.

3.3. - Chamber Construction

We are building two test chambers, each having a 24-wire anode plane centered between 2 cathode planes 1.5 mm apart. (See Fig. 5 schematic.) The anode planes are an array of 5-μ-diameter tungsten wires spaced 20 μ apart, stretched across a 3-mm-diameter hole in a 0.5-mm-thick, 19-mm-diameter

ceramic washer. (See Fig. 6b and c). Two 250-μ-diameter plastic rods were tightly wound with 20-μ-diameter formvar-coated copper wire and glued to the ceramic on each side of the hole, providing a series of sharp grooves to guide the winding of the 5-μ wire. Note that after winding, the 5-μ wires were approximately 250 μ above the ceramic surface. The 24 5-μ wires were spot-welded to 24 pads of silver paint located at the edge of the ceramic disk (visible in Fig. 6b). The chamber body was machined from a pair of standard 2.75-inch Varian Conflat Flanges. (See Fig. 6a.) A copper gasket seals the two flanges as they are bolted together. Three glass-to-kovar feed-throughs were welded to one flange. Each feed-through contains eight kovar wires that pass into the chamber where they are connected to the silver pads.

For chambers having several hundred wires, the feed-through problem must be re-evaluated. The description above serves only as an example of how a number of closely spaced wires can be handled.

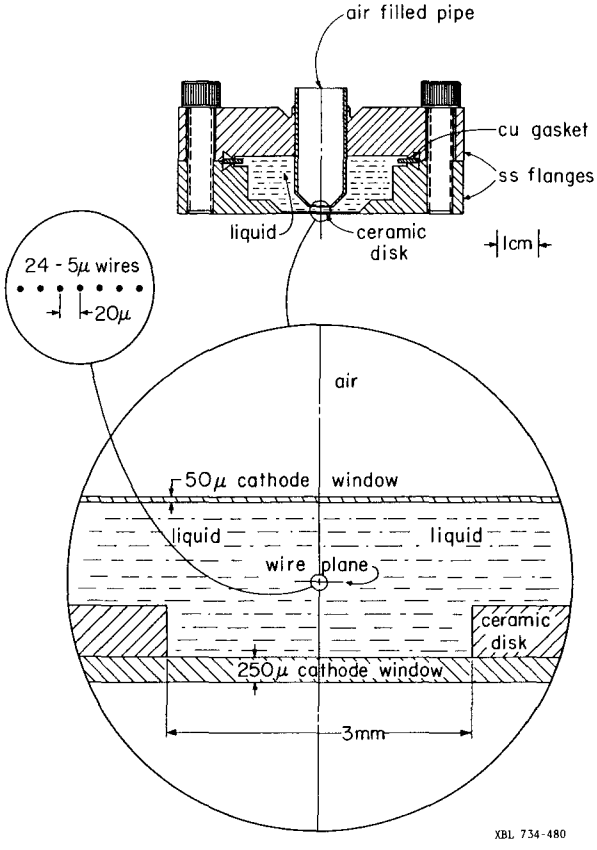

Fig. 5. Cut-away drawing of high-resolution liquid-filled multi-wire ionization chamber. Upper drawing shows assembled flanges and air-filled pipe to reduce the amount of material in the beam. Enlargement below (25X relative to top drawing) shows cathodes, ceramic disk, anode plane, and liquid. Detail at left (250X relative to top drawing) shows wire array.

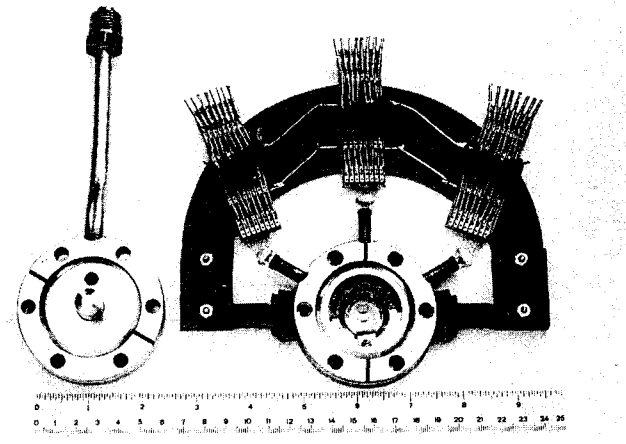

Fig. 6a. Photograph of the chamber sketched in Fig. 5. Flange at left shows vacuum and fill pipe. Flange at right shows ceramic disk and three 8-conductor feed-throughs. The printed circuit boards contain capacitors and resistors to allow the anode wires and charge amplifiers to operate at different potentials.

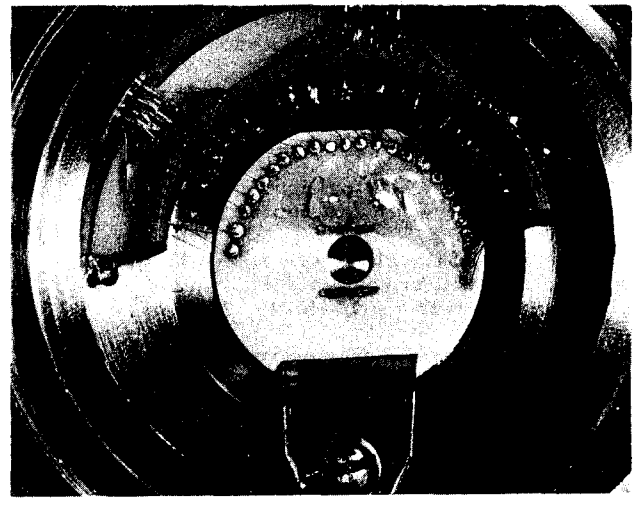

Fig. 6b. Close-up of ceramic disk and feed-throughs. Note wires stretched across center of hole. Scale is 5X relative to Fig. 6a.

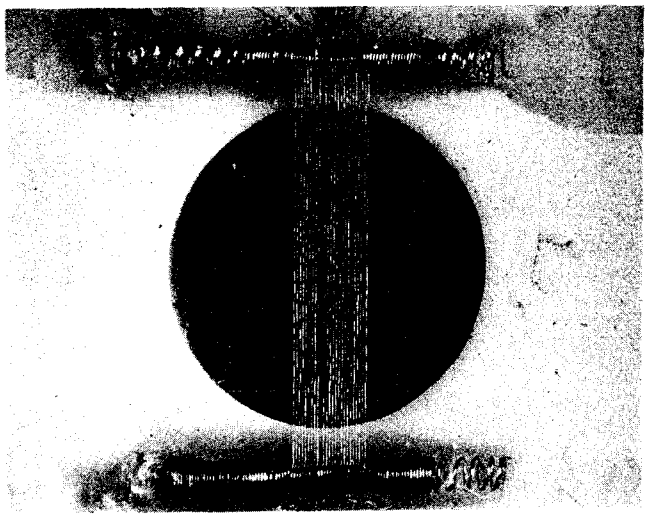

Fig. 6c. Close up of chamber wires and winding guides. Note missing wire. Scale is 31X relative to Fig. 6a.

3.4. -Readout

We are currently building arrays of charge amplifiers to be used both for the high-resolution chambers and the gamma-ray cameras. A block schematic is shown in Fig. 7. The field effect transistors (FETs) are located near the chamber to take advantage of the lower noise level at -107°C. The noise level is typically ±800 e^- at 2 μs rise time and ±1300 e^- at 100 ns rise time. The latter noise figure is equivalent to 7 μV rms at the input of the FET.

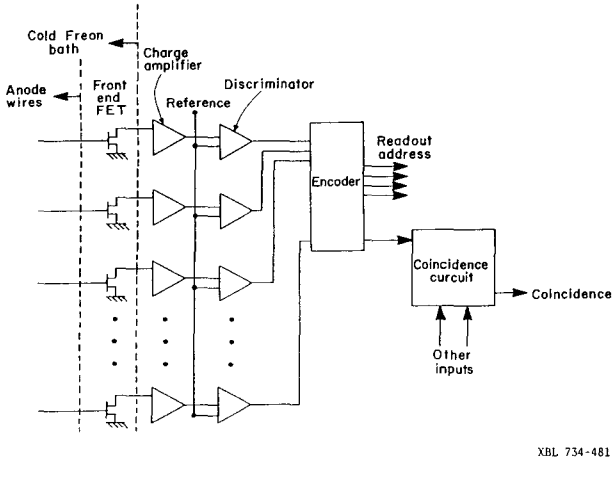

Fig. 7. Schematic of readout, using one amplifier per line. FETs are mounted on chamber and are thus cooled to reduce noise. Charge amplifiers and discriminators are located nearby.

The FET and the associated components are spaced 8 mm apart and mounted directly on the chamber on a printed circuit board. This section is estimated at $2.00 per wire. The charge amplifiers (including the discriminators) are spaced 3 cm apart and placed on a printed circuit board. This assembly is mounted in an electronic rack near the chamber. The estimated cost of parts for this assembly is $12.00 per channel.

ACKNOWLEDGMENTS

We are indebted to Joseph Savignano, Charles Taylor, Tony Vuletich, and Buck Buckingham for their skill and patience in building and maintaining our equipment. We are grateful to Philippe Eberhard, Gary Chanan, Terry Mast, and Richard Muller for many helpful discussions.

This work was supported by the U. S. Atomic Energy Commission.

Footnotes and References

1. L. W. Alvarez, Lawrence Radiation Laboratory, Group A Physics Note No. 672, 1968 (unpublished).

2. R. Muller, S. E. Derenzo, G. Smadja, D. B. Smith, R. G. Smits, H. Zaklad, and L. W. Alvarez, Phys. Rev. Letters 27, 532 (1971).

3. S. E. Derenzo et al., Proceedings XVI International Conference on High Energy Physics, Chicago-Batavia, Illinois, 2, 388 (1972).

4. H. Zaklad, S. E. Derenzo, R. A. Muller, G. Smadja, R. G. Smits, and L. W. Alvarez, Trans. IEEE NS-19, No. 3, 206 (1972).

5. H. Zaklad, S. E. Derenzo, R. A. Muller, and R. G. Smits, Trans. IEEE NS-20 No. 1, 429 (1973).

6. S. E. Derenzo, D. B. Smith, R. G. Smits, H. Zaklad, L. W. Alvarez, and R. A. Muller, Lawrence Radiation Laboratory Report UCRL-20118, NAL Summer Study Report SS-181, p. 45 (1970).

7. Haim Zaklad (D. Eng. thesis), Lawrence Radiation Laboratory Report UCRL-20690 (1971).

8. S. Derenzo, T. S. Mast, R. A. Muller, and H. Zaklad, Lawrence Berkeley Laboratory Report LBL-1313 (1973), submitted to Phys. Rev.

9. A. A. Kruithof, Physica 7, 519 (1940).

10. S. G. S. Louie, Lawrence Berkeley Laboratory Group A Physics Note 765 (1973).

11. A. F. Pisarev, V. F. Pisarev, and G. S. Revenko, Dubna Report JINR-P1 3-6449 (to be published in JETP).

12. A. F. Pisarev, V. F. Pisarev, and G. S. Revenko, Dubna Report JINR-P13-6450 (to be published in JETP).

13. D. W. Swan and T. J. Lewis, Proc. Phys. Soc. 78, 448 (1961).

14. In a multi-wire proportional chamber, the cathode field is given quite accurately by:

$$E_c = \frac{V/b}{[1+(\frac{s}{\pi b}\ln(\frac{s}{2\pi\rho})]},$$

where V is the applied voltage, s the wire spacing, ρ the wire radius, and 2b the chamber thickness. The average anode field E_a is related to E_c by:

$$\frac{E_a}{E_c} = \frac{s}{\pi\rho},$$

an equation easily remembered by considering that the field lines covering a region s at the cathode must concentrate to a region πρ at the anode. These expressions were derived from the more general equations given in P. M. Morse and H. Feshbach, Methods of Theoretical Physics, Vol. II, Chap. 10 (McGraw-Hill, New York, 1953). For an extensive analysis of fields in multi-wire chambers, including many graphs, see G. Chanan, Lawrence Berkeley Laboratory Group A Physics Note No. 770, 1973.

15. H. H. Staub, Experimental Nuclear Physics, Vol. I, edited by E. Segrè (John Wiley, New York, 1952), p. 16.

16. L. S. Miller, S. Howe, and W. E. Spear, Phys. Rev. 166, 871 (1968).

17. G. A. Cook, editor, Argon, Helium, and the Rare Gases (John Wiley, New York, 1961).

18. R. E. Shuping, C. R. Phillips, and A. A. Moghissi, Radiological Health Data and Reports 11, 671 (1970).

19. F. Crawford, Lawrence Radiation Laboratory Report UCID-241 (1957); also B. Rossi, High Energy Particles (Prentice-Hall, New York, 1952), p. 138.

20. L. Miller, Lawrence Berkeley Laboratory, Group A Physics Note No. 769 (1973).

21. R. W. Warren and J. H. Parker, Jr., Phys. Rev. 128, 2661 (1962). Several basic diffusion equations are given in B. B. Rossi and H. H. Staub, Ionization Chambers and Counters (McGraw-Hill, New York, 1949), p. 18.

22. S. E. Derenzo, D. Anderberg, S. Buckingham, R. A. Muller, R. G. Smits, J. Savignano, T. Vuletich, and H. Zaklad, Lawrence Radiation Laboratory Report UCRL-20857 (1971).